Accepted Manuscript

Identification of small-molecule inhibitors of USP2a

Marcin D. Tomala, Katarzyna Magiera-Mularz, Katarzyna Kubica, Sylwia Krzanik, Bartosz Zieba, Bogdan Musielak, Marcin Pustula, Grzegorz M. Popowicz, Michael Sattler, Grzegorz Dubin, Lukasz Skalniak, Tad A. Holak

PII: S0223-5234(18)30244-7

DOI: 10.1016/j.ejmech.2018.03.009

Reference: EJMECH 10274

To appear in: *European Journal of Medicinal Chemistry*

Received Date: 24 October 2017

Revised Date: 15 February 2018

Accepted Date: 1 March 2018

Please cite this article as: M.D. Tomala, K. Magiera-Mularz, K. Kubica, S. Krzanik, B. Zieba, B. Musielak, M. Pustula, G.M. Popowicz, M. Sattler, G. Dubin, L. Skalniak, T.A. Holak, Identification of small-molecule inhibitors of USP2a, *European Journal of Medicinal Chemistry* (2018), doi: 10.1016/j.ejmech.2018.03.009.

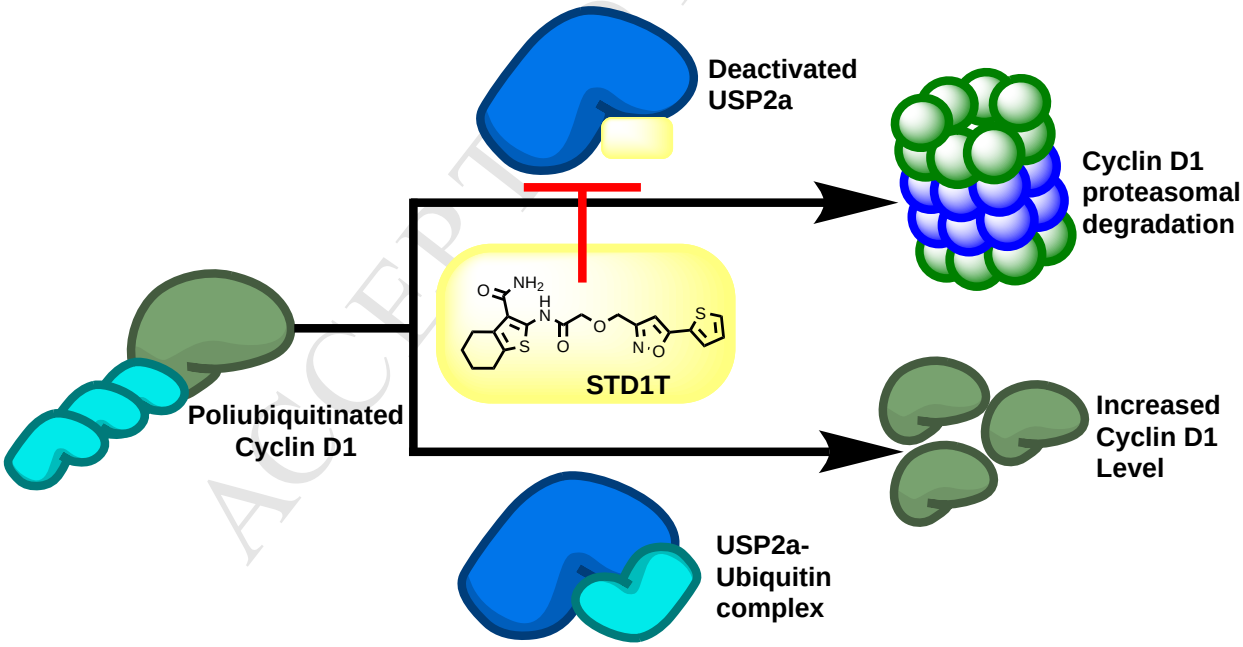

Identification of small-molecule inhibitors of USP2a

Marcin D. Tomala[1], Katarzyna Magiera-Mularz[1], Katarzyna Kubica[1], Sylwia Krzanik[2], Bartosz Zieba[2], Bogdan Musielak[1], Marcin Pustula[1], Grzegorz M. Popowicz[3], Michael Sattler[3], Grzegorz Dubin[2], Lukasz Skalniak[1] & Tad A. Holak[1*]

[1] Faculty of Chemistry, Jagiellonian University, Gronostajowa 2, 30-387 Krakow, Poland

[2] Faculty of Biochemistry, Biophysics and Biotechnology, Jagiellonian University, Gronostajowa 7, 30-387 Krakow, Poland

[3] Institute of Structural Biology, Helmholtz Zentrum München, Ingolstädter Landstrasse 1, 85764 Neuherberg, Germany

* holak@chemia.uj.edu.pl

ABSTRACT

USP2a is a deubiquitinating protease that rescues its target proteins from destruction by the proteasome by reversing the process of protein ubiquitination. USP2a shows oncogenic properties *in vivo* and has been found to be a specific activator of cyclin D1. Many types of cancers are addicted to cyclin D1 expression. Targeting USP2a is a promising strategy for cancer therapy but little progress has been made in the field of inhibition of USP2a. Using NMR-based fragment screening and biophysical binding assays, we have discovered small molecules that bind to USP2a. Iterations of fragment combination and structure-driven design identified two 5-(2-thienyl)-3-isoxazoles as the inhibitors of the USP2a-ubiquitin protein-protein interaction. The affinity of these molecules for the catalytic domain of USP2a parallels their ability to interfere with USP2a binding to ubiquitin *in vitro*. Altogether, our results establish the 5-(2-thienyl)-3-isoxazole pharmacophore as an attractive starting point for lead optimization.

Keywords:

Deubiquitinase, ubiquitin, small-molecular inhibitors, heterocyclics, anticancer

1. Introduction

USP2a is a cysteine protease and a member of the ubiquitin-specific protease family (USP) [1–3]. The USPs constitute the largest family of a superfamily of about 100 deubiquitinases (DUBs). DUBs specifically remove the ubiquitin tag from ubiquitinated proteins that are meant for destruction by the proteasome and thus prevent their proteasomal degradation. USP2a has been identified as a specific DUB of MDM2 (an inhibitor of p53) [4–6], fatty acid synthase [7], Cry1 (proteins involved in the

circadian rhythm) [8], and cyclin D1 [9]. The tumorigenesis of several types of cancer is linked to overexpression of cyclin D1. USP2a directly interacts with cyclin D1 and inhibits its ubiquitin-dependent degradation. This leads to the promotion of cyclin D1 stabilization that may induce growth of cancer cells depended on the expression of cyclin D1 [9].

USP2a is upregulated in various cancers [7]; for example, it is overexpressed in prostate cancer. Stabilization of the fatty acid synthase by USP2a has been associated with the malignancy of some aggressive prostate [10], breast and ovarian cancers [11–13]. In addition, USP2a itself has oncogenic properties *in vivo* and *in vitro* that are linked to its proteolytic activity [10]. The inhibition of the proteolytic activity of USP2a offers a new strategy for protein-directed therapies in the treatment of cancer. The structure of the complex of USP2a and ubiquitin (Ub) was solved in 2006 [14]. Nevertheless, finding promising candidates for effective inhibitors of USP2a is still in its initial stadium [15,16]. Herein, we report the identification of small-molecule inhibitors of USP2a. These molecules provide the starting lead for further design and development of more potent inhibitors of the USP2a-Ub axis.

2. Results

2.1. Saturation transfer difference (STD) NMR screening for fragments

The Maybridge Ro3 Diversity Fragment Library, consisting of 1500 small-molecule compounds, was screened for their binding to USP2a using the saturation transfer difference (STD) NMR experiments [17]. Eleven compounds were selected that showed the binding to USP2a (Table 1). Examples of the ^{1}H STD-NMR experiments are shown in Fig. 1 and related negative controls in Fig. S1 in the Supplementary Information.

Table 1. The effects of small organic fragments on the activity of USP2a

Compound name	**Structure**	**Ub-AMC assay IC_{50} [mM]**
STD1	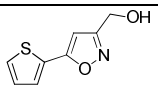	1.3 ± 1.1
STD2	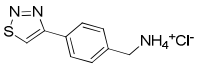	> 5
STD3	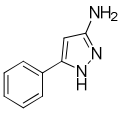	> 5
STD4	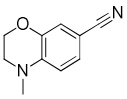	not active
STD5	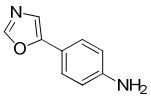	undefinable*
STD6	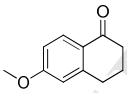	undefinable*
STD7	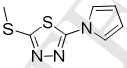	undefinable*
STD11	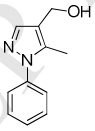	not active
STD12	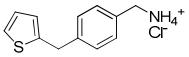	not active
STD13	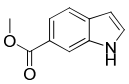	fluorescent activity
STD14	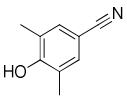	> 5

*for the indicated compounds the IC_{50} values were undefinable due to the increase of solution turbidity at higher concentrations of the compounds.

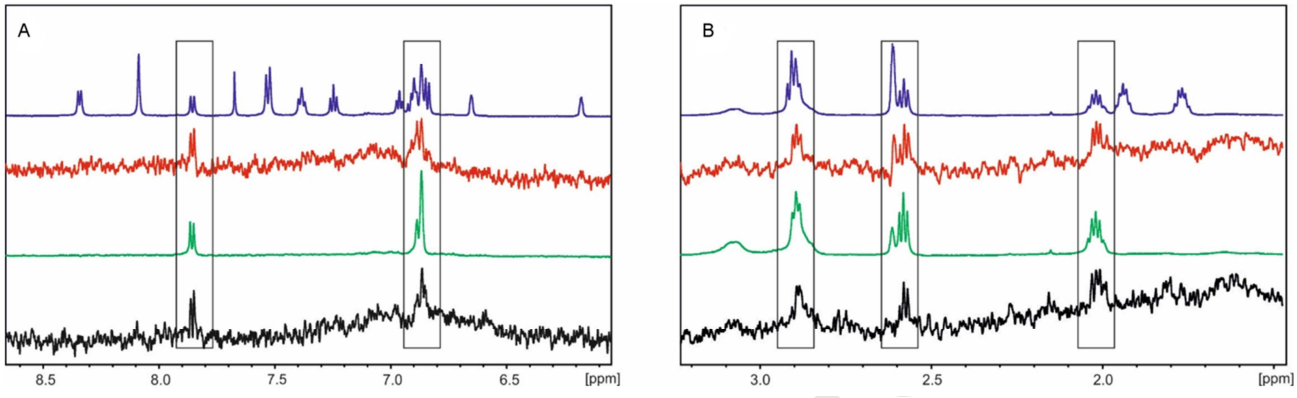

Fig. 1. STD NMR screening of fragments for USP2a. (A) Aromatic and (B) aliphatic part of the spectrum. Blue: The ^{1}H NMR spectrum of the mixture of five fragments. Red: The STD ^{1}H NMR spectrum of the mixture. Green: The ^{1}H NMR spectrum of fragment STD1, Black: The STD ^{1}H NMR spectrum of fragment STD1. Identical resonances appear on STD spectra for both mixture and a single compound alone. They overlap with ^{1}H signals of compound STD1.

2.2. Verification of STD hits for their activity towards the USP2a protein

To verify the capability of the fragments to inhibit the enzymatic activity of USP2a, we used Ub-AMC hydrolysis assay. This *in vitro* assay is based on the ubiquitin (Ub) C-terminal 7-amido-4-methyl-coumarin (AMC) substrate which is hydrolyzed by active DUB enzymes. During the enzymatic reaction, the fluorescent dye AMC is released from the quencher. This causes the increase of the fluorescent signal and allows to measure the activity of the enzyme by fluorescence spectroscopy [18].

Activities of 11 fragments were tested using an isolated USP2a enzyme after the incubation at various concentrations of potentially active compounds. Seven of the tested small-molecule compounds showed the capability to inhibit the activity of USP2a (Table 1). The best compound, STD1, inhibited the enzymatic activity of USP2a with the IC_{50} value 1.3±1.1 mM and had good solubility in the assay conditions.

To verify the potential of the STD1 compound, we have performed a 4-step binary NMR titration experiment [19] in which we used a constant amount of USP2a and increasing amounts of STD1 (Fig. 2).

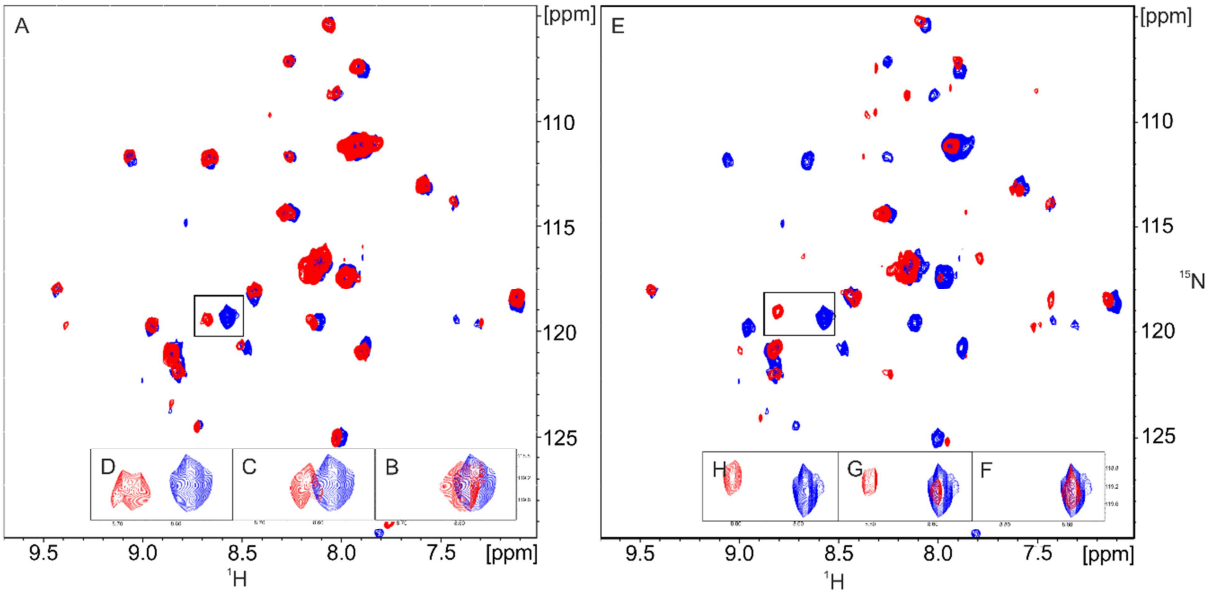

Fig. 2. ^{1}H-^{15}N HSQC spectra of the selectively ^{15}N-Gly, ^{15}N-Cys, ^{15}N-Ser and ^{15}N-Trp labeled USP2a, which depicts changes in chemical shifts after the addition of compound STD1. (A) The reference spectrum of apo-USP2a (blue) superimposed with the spectrum of USP2a after the addition of the inhibitor in the protein:compound molar ratio of 1:15 (red). (B, C, D) The enlarged cross-peaks, that indicate the binding of STD1 to USP2a. (B) USP2a:STD1 at the molar ratio 1:1, (C) 1:5 and (D) 1:15, respectively. (E) Reference spectrum of apo-USP2a (blue) superimposed with the spectrum of USP2a (red) overtitrated with unlabeled ubiquitin (Ub). (F, G, H) The enlarged cross-peaks representing the titration steps: (F) USP2a:Ub at the molar ratio 4:1, (G) USP2a:Ub 2:1 and (H) USP2a:Ub 1:1. For (G) two separate sets of ^{1}H-^{15}N HMQC resonances are observed, one corresponding to the free USP2a and the other to the USP2a bound to Ub. This demonstrates that the USP2a/Ub complex on the NMR chemical shift time scale [19].

NMR confirmed the binding of this fragment compound to USP2a with $K_D = 0.9 \pm 0.3$ mM, which is comparable to the value of the IC_{50} established by the Ub-AMC hydrolysis assay. In addition, the data show that NMR peaks that shift upon the STD1 binding are the same as those affected by the binding of

ubiquitin (insets in Fig. 2A and 2E). Additionally, the affinity of the STD1 compound was confirmed by the NMR competition binding experiment using the AIDA-NMR measurements [20] (Fig. S2). The AIDA-NMR indicates that STD1 dissociates the Ub/USP2a complex. An additional portion of Ub has not caused the changes in the spectrum indicating that STD1 competes with ubiquitin for the binding to USP2a.

For compounds STD5, STD6, STD7, some activity towards the USP2a protein has been noticed. However, the turbidity of the solutions (monitored during the assay showed at higher concentrations of the compounds) did not allow for determining the IC_{50} values in the Ub-AMC assay. To clear out this result the 4-step binary NMR titration experiment was performed for these compounds, revealing no binding to USP2a (as shown, for example, for STD5 in Fig. S1B). Therefore, the compounds were classified as false positives in the STD NMR experiment.

For the compounds STD2, STD3, STD14 a weak activity has been observed (with IC_{50} values above 5 mM) and these compounds were not considered as proper candidates for binding fragments to USP2a. The use of the Ub-AMC hydrolysis assay was impossible for the STD13 compound due to its fluorescent properties. The remaining three compounds were not active in the Ub-AMC experiment.

2.3. Expanding the active fragment

To expand on our most active STD1 hit, we tested commercially available derivatives of this fragment. We tested five compounds STD1B, STD1C, STD1M, STD1P, and STD1T by using the Ub-AMC hydrolysis assay (Table 2).

Table 2. The effects of the STD1 derivatives on the activity of USP2a

Compound name	**Structure**	**IC_{50} [μM] (Ub-AMC assay)**
STD1B	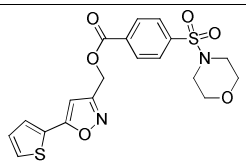	not active
STD1C	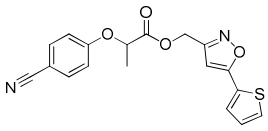	> 50
STD1M	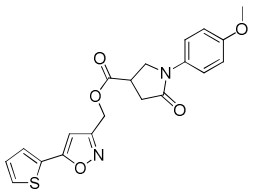	not active
STD1P	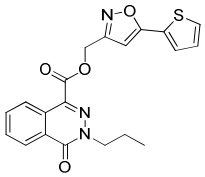	> 100
STD1T	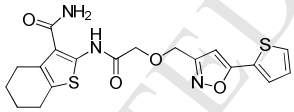	3.3 ± 1.1

Three of the tested compounds showed activity towards USP2a (Table 2). For the most potent STD1T we observed the IC_{50} value of 3.3 μM, a huge one-thousand-fold increase of the inhibition compared to the initial STD1 fragment (Table 2, Fig. 3).

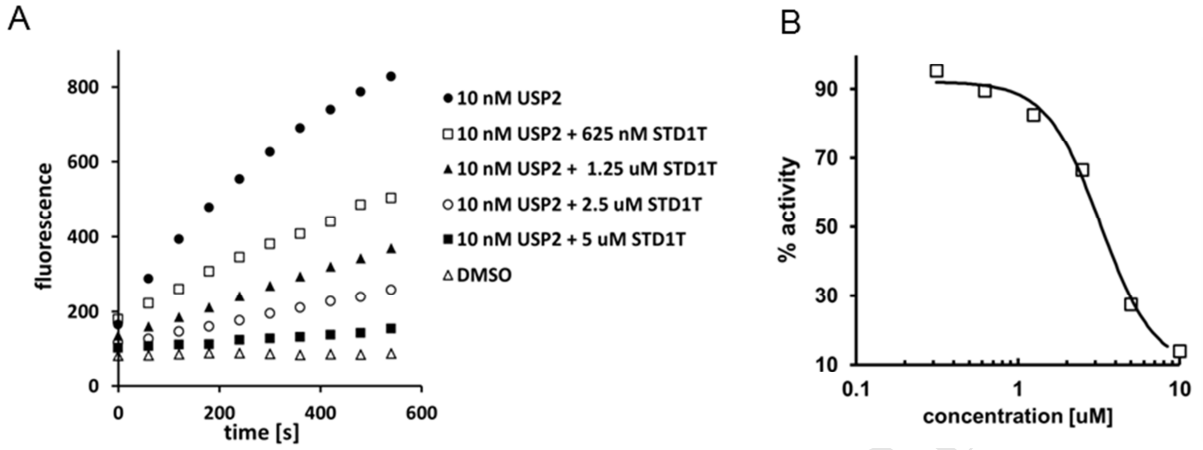

Fig. 3. The Ub-AMC hydrolysis assay of USP2a activity. (A) STD1T compound inhibits USP2a enzymatic activity in a concentration dependent manner. (B) A dose-response inhibition of USP2a activity measured in the Ub-AMC hydrolysis assay, in the presence of various concentrations of STD1T.

The compounds STD1C and STD1P showed some activities with IC_{50} values above 50 μM. The rest of the compounds were not active.

The data in Table 2 indicate that the greatest potential lies in the compound STD1T. The retroanalysis of the STD1T structure encouraged us to perform synthesis of a benzothiophene fragment STG3 which is part of the structure of STD1T (Table S1). For STG3, we observed the IC_{50} value of 8.7 μM, which indicates that this STD1T fragment may be the one responsible for the strong activity of STD1T in the Ub-AMC assay. Furthermore, we attempted to optimize the physical properties of the STD1T compound, focusing mostly on its water solubility. This issue is discussed in Table S1 of the Supplementary Information.

In order to investigate the possible binding mode of the STD1T compound, we performed the simple docking of the molecule assuming that the molecule binds in the area naturally occupied by the ubiquitin C-terminus (Fig. S3). The STD1T molecule is likely to create a number of hydrogen bonds

with Gln 294, Gly 463 and His 456 of USP2a. The proximity of the thiophene ring and –SH substituent of the active Cys 223 could be the possible source of additional covalent interactions [21].

Additionally, to give the insight into the selectivity of our leading structure, we performed the Ub-AMC hydrolysis affinity test against the USP7 protease, the deubiquitinase that is closely related to USP2a in terms of its amino acid sequence and the global structure. Both STD1T and STD1 showed selective inhibition of USP2a vs. USP7 at the concentrations of 10 μM and 2000 μM, respectively (Fig. 4).

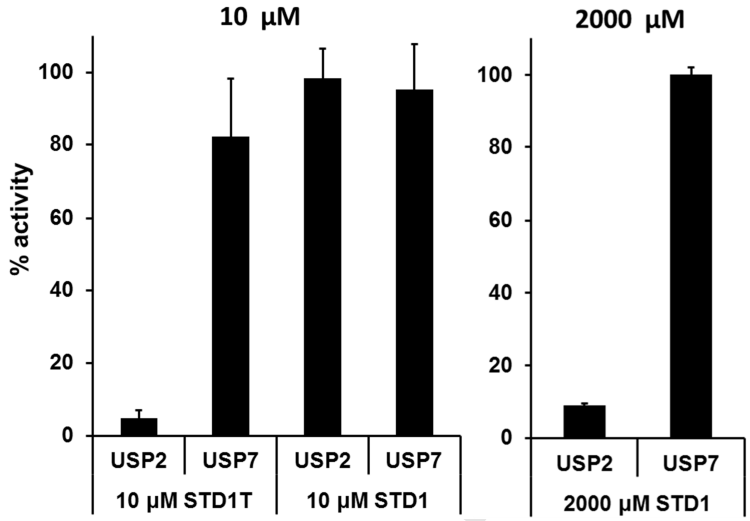

Fig. 4. Effects of the compounds STD1 and STD1T on the activity of USP2a and USP7 proteins.
The graphs present the comparison of the inhibitory potential of the compounds towards the two deubiquitinases tested in the Ub-AMC hydrolysis assay. STD1T and STD1 compounds show a greater affinity to USP2a protein than to the USP7 at the tested concentrations. The graphs show mean ± SD values.

To verify the bioactivity of the optimized STD1T compound and compare its potential to STD1 precursor both compounds were used in a cell-based model. Based on the report of Shan and co-workers [9] we have tested the influence of the compounds on the expression of cyclin D1. Cyclin D1 was suggested to be stabilized by USP2a and thus can be used to track the activity of USP2a in cells.

HCT 116 and MCF-7 cells were treated with 20 µM of the compounds, or with the equivalent portion of DMSO. The cells were cultured for 48 hours and subjected to western blot hybridization. A down-regulation of cyclin D1 expression was observed in the cells treated with STD1T, as compared to DMSO-treated controls (Fig. S4). STD1 did not change the expression of cyclin D1(Fig. S4). This result supports the inhibitory potential of STD1T towards USP2a.

3. Discussion

NMR spectroscopy is a highly versatile screening method for drug discovery [22–24]. In comparison with other screening technologies, a unique advantage of NMR is its robust capability to detect weak mM intermolecular interactions. This renders NMR as an ideal method for fragment-based screening, where detection of binding between low-affinity fragments and target proteins is studied [23,25–30]. Among NMR methods, the ligand-observed saturation transfer difference (STD) experiment has a number of advantages compared to protein-observed NMR experiments: the protein requirement is much lower, there is no need for labeling, and there is no size limitation for the protein [23,25,31]. These features have particular significance in the case of USP2a due to the relatively large size of the protein (347 amino acids) and the low expression yield of the recombinant USP2a; therefore, we decided to apply this technique for screening the Maybridge Ro3 Diversity Fragment Library of 1500 chemical fragments. We identified 11 compounds that showed bidding affinity towards USP2a as the result of our screen (Table 1). The most promising STD NMR result among these compounds was observed for the STD1.

While the STD NMR approach is widely used for fragment screening, the method has one drawback: the technique identifies both specific and nonspecific binders due to its capability to accumulate binding signal from multiple binding sites. Consequently, after the STD-based screening campaign, it is necessary to discriminate between specific and nonspecific binders by, for example,

performing competition STD experiments [32]. The competitive binders must have a high affinity or a high solubility in order to efficiently displace the fragment. When such competitive reference compounds are not available, an orthogonal biochemical assay is required to validate the fragment hit. We used the latter approach in that we checked the activities of the compounds with the Ub-AMC hydrolysis assay. The highest Ub-AMC activity was obtained for our clearest hit in the STD NMR, compound STD1, which showed the IC_{50} of 1.3 mM. Extension of this scaffold produced the hit-to-lead USP2a inhibitor (STD1T) with the inhibition affinity of 3.3 µM. The compound presents promising biological activity, as shown by the analysis of the expression of USP2a-regulated cyclin D1 in two human cell lines.

4. Conclusion

Using NMR-based fragment screening and a biochemical binding assay, we have discovered small molecules that bind to USP2a. Iterations of fragment combination and structure-driven design identified two 5-(2-thienyl)-3-isoxazoles as the inhibitors of the USP2a-ubiquitin protein-protein interaction. The affinity of these molecules for the catalytic domain of USP2a parallels their ability to interfere with the *in vitro* hydrolysis of ubiquitin-AMC by USP2a. This establishes the STD1/STD1T 5-(2-thienyl)-3-isoxazole pharmacophore as an attractive starting point for further lead optimization. The scaffold shows a clear hydrolysis-inhibitory specificity for USP2a compared to USP7, the deubiquitinase similar to USP2a in amino acid sequence and structure.

5. Experimental section

5.1. Expression and purification of ubiquitin

Escherichia coli BL21 (DE3) strain cells (Invitrogen) were transformed with pet16b-UBwt (1-76, human) and grown in LB medium supplemented with 100 µg/ml ampicillin at 37 °C. The expression of the protein was induced with 1 mM IPTG at an OD_{600} of 0.7-0.9 and the bacteria were grown for additional 6 h at 37 °C. The cells were harvested by centrifugation and frozen at -20 °C. Ubiquitin purification was carried out according to the optimized protocol[33]. The cells from 4 L cell culture were resuspended in 200 ml of lysis buffer (50 mM NaH_2PO_4 pH=8.0, 300 mM NaCl, 1 mM imidazole) to which 1 mg/ml of lysozyme was added. After the incubation of the cells on ice (10 min), NaCl and PMSF were added to final concentrations 600 mM and 2 mM, respectively. The cells were raptured by sonication and after centrifugation the supernatant was loaded on a Chelating Sepharose Fast Flow (GE Healthcare) which has been charged with 0.2 M $NiSO_4$. The column was washed consecutively with lysis buffer (50 ml), lysis buffer without NaCl (15 ml), lysis buffer adjusted to pH=5.5 (30 ml) and pH=4.5 (50ml). The protein was eluted with lysis buffer supplemented with 250 mM imidazole.

As the last purification step the sample was loaded on the size exclusion chromatography column HiLoad 16/60 Superdex 75 prep grade (GE Healthcare) which has been equilibrated with PBS pH=7.4 buffer. The ubiquitin was stored as 1 ml aliquots at the concentration of 0.5-2 mM protein at -20 °C, or freshly used for the measurements.

5.2 USP2a protein expression and purification

Human USP2a (residues 258-605) was cloned into the pET21a vector and expressed in the *E. coli* BL21 (DE3, Invitrogen). The cells were grown in LB medium containing 100 µg/ml ampicillin at 37 °C and induced with 0.5 mM IPTG at OD_{600} of 0.7-0.9. The bacteria were cultured for additional 5 h at 37 °C. The cells were harvested by centrifugation and frozen at -20 °C. USP2a purification was carried out according to optimized protocol ([14]). In brief, the cells from 6 L culture were resuspended in 300 ml of lysis buffer (10 mM Tris/HCl pH=8.0, 1 mM $MgCl_2$, 5 mM β-mercapthoetanol, 10 µM PMSF) and

ruptured by sonication. After the centrifugation supernatant was loaded on a Chelating Sepharose Fast Flow (GE Healthcare) charged with nickel ions. The column was washed with lysis buffer and protein was eluted with lysis buffer supplemented with 250 mM imidazole. Fractions containing USP2a were combined and further purified on Q-Sepharose Fast Flow (GE Healthcare) column. USP2a protein was in the flow-through fraction.

As the last purification step the sample was loaded on the size exclusion chromatography column HiLoad 16/60 Superdex 75 prep grade (GE Healthcare). During the preparation of USP2a protein for Ub-AMC assay experiments, gel filtration column has been equilibrated with PBS pH 7.4, 5 mM DTT buffer. The final USP2a samples were stored as 20 µl aliquots at the concentration of 0.01 mM protein in a buffer containing 10% glycerol at -80 °C. For the preparation of USP2a sample for STD-NMR experiments, gel filtration column has been equilibrated with PBS pH 7.4, 1 mM DTT buffer (instead of 5 mM) and the final USP2a sample was freshly used for the experiments.

5.3. USP7 expression and purification

Human USP7 catalytic domain (residues 208-561) was cloned into the pGEX-6P-1 vector (GE Healthcare) and expressed in the E. coli BL21 (DE3, Invitrogen). Cells were grown in LB medium containing 100 µg/ml ampicillin at 37°C and induced with 0.5 mM IPTG at OD_{600} of 0.7-0.9 and cultured overnight at 16°C. Cells were harvested by centrifugation. Next cells were resuspended in buffer A (50 mM Tris/HCl pH 9.0, 50 mM NaCl, 3 mM β-mercapthoetanol) and disrupted by sonication. Cell lysate was clarified by centrifugation (45 000 g, 40 min.) and dialyzed against buffer A.

The supernatant was loaded onto Q-Sepharose column and proteins were eluted with NaCl gradient. Fractions containing GST fused USP7 were combined, concentrated and dialyzed against buffer (50 mM Tris/HCl pH 7.0, 50 mM NaCl, 3 mM β-mercapthoetanol). During dialysis protein was digested

with PreScission Protease (GE Healthcare). USP7 protein and cleaved GST were separated on Mono Q HR 10/10 column (GE Healthcare). The last purification step consisted of size exclusion chromatography on HiLoad 16/60 Superdex 75 prep grade (GE Healthcare) in 50 mM Tris/HCl, 150 mM NaCl, 2 mM DTT.

5.4. Selectively labeled ^{15}N-Gly, ^{15}N-Cys, ^{15}N-Ser and ^{15}N-Trp USP2a: expression and purification

A sample of ^{15}N selectively labeled USP2a with the ^{15}N-glycine, ^{15}N-cysteine, ^{15}N-serine and ^{15}N-tryptophan was prepared according to the procedure described by Li and Hoffman, 2001. The *E. coli* strain cells were grown in the defined medium containing unlabeled ammonium chloride, 400 mg/l ^{15}N-glycine, no serine, no cysteine, and no tryptophan and the residual 16 unlabeled amino acids in the corresponding concentrations (400 mg/l Ala, Glu, Gln, Arg, Ile, Val; 255 mg/l Asp; 125 mg/l Met; 100 mg/l Asn, Leu, Lys, His, Pro, Thr, Tyr; 50 mg/l Phe). The expression and purification of such a labeled protein was performed according to the protocol described above for the expression and purification of the unlabeled USP2a. After the gel filtration, USP2a protein was concentrated to 0.2-0.3 mM and freshly used for the NMR measurements.

5.5. The Ub-AMC hydrolysis assay

Deubiquitination assay was performed using Infinite 200 PRO – Tecan plate reader and 96-well, black Greiner microplates in a 100 µl reaction volume. DUBs activity assay was performed in the reaction buffer 50 mM Tris/HCl, pH=7.5, 1 mM EDTA, 1 mM $MgCl_2$ by incubating USP2a enzyme (10 nM) with the excess of tested compounds for 30 min. The fluorescence was measured at 30 s intervals, at excitation and emission wavelengths of 355 nm and 460 nm respectively, immediately after the substrate Ub-AMC (500 nM, Viva Biosience) was added [18]. In order to check the solubility of the

assay components, the turbidity of the assay solution was monitored by measuring the absorbance at the 600 nm wavelength. The values were referenced to the absorbance value (of 0.043) of the mixture of 500 nM Ub-AMC, 10 nM USP2a and 1% DMSO in the assay buffer. Absorbance above 0.050 indicated precipitation and the data were evaluated.

The excess of wild-type ubiquitin was used as a positive control. To obtain dose-response curves, the percent of the enzyme inhibition was first calculated and then the curve fitting was performed.

5.6. NMR experiments

All NMR experiments were recorded on a Bruker Avance 600 MHz spectrometer equipped with a triple resonance cryoprobe head and an automated SampleJet sample changer. The samples for STD-experiments were prepared in PBS buffer at pH 7.4 in D_2O. STD-NMR experiments were performed for 40:1 USP2a: compound molar ratios at 298 K.

The STD-NMR[22,23,25,34] spectra were acquired with 320 transients of 16 K data points in a spectral window of 12019.23 Hz centered at the water signal with 1.5 s relaxation delay between the scans. Water suppression was carried out using the WATERGATE sequence[35]. Selective saturation of the protein resonances (on resonance spectrum) was performed by irradiating at −0.5 ppm using a series of Eburp2.1000-shaped 90° pulses (50 ms, 1 ms delay between pulses) for a total saturation time of 2.0 s. For the reference spectrum (off resonance), the samples were irradiated at 10 ppm. On- and off-resonance scans were subtracted using phase cycling. Control experiments were performed with the ligands in the presence and absence of USP2a in order to optimize the frequency of protein saturation (−0.5 ppm) and to ensure that the ligand signals were not affected. The fragment library screening was performed by testing 300 mixtures containing five fragments each initially. Mixtures that yielded positive STD signals were selected and deconvolved, i.e. fragments that formed “active” mixtures were

tested separately. Positive hits were further tested by STD experiment without USP2a to exclude false positives.

The selectively ^{15}N-labeled USP2a for the binary titration was obtained from gel filtration in PBS (pH 7.4) with 5 mM DDT buffer. To provide lock signal 10% (v/v) D_2O was added. Stock solutions of inhibitor used for titration were prepared in d_6-DMSO with final concentration 50mM. The spectra were processed with TopSpin 3.2 software. The NMR titration was performed as three step experiment with the compound to protein complex ratio 1:1, 1:5 and 1:15.

5.7. Molecular docking

Models of molecules STD and STD1T interacting with presumed USP2a hot spot were prepared according to simple docking operations. As a model core we used the X-Ray structure (2HD5) of ubiquitin and USP2a complex [14], all ligands, including water molecules, ions were removed. The geometries of ligands were optimized with the application of Avogadro [36] . Ligands were set in degrees of rotation and the receptor was provided with polar hydrogens, all the files were converted to pdbqt files in AutoDockTools (ADT). The Calculations were performed in AutoDock4 with the application of Lamarckian Genetic Algorithm [37].

References

[1] D. Komander, M.J. Clague, S. Urbé, Breaking the chains: structure and function of the deubiquitinases, Nat. Rev. Mol. Cell Biol. 10 (2009) 550–563.

[2] D. Komander, M. Rape, The Ubiquitin Code, Annu. Rev. Biochem. 81 (2012) 203–229.

[3] M.J. Clague, I. Barsukov, J.M. Coulson, H. Liu, D.J. Rigden, S. Urbé, Deubiquitylases from genes to organism, Physiol. Rev. 93 (2013) 1289–1315.

[4] L.F. Stevenson, A. Sparks, N. Allende-Vega, D.P. Xirodimas, D.P. Lane, M.K. Saville, The deubiquitinating enzyme USP2a regulates the p53 pathway by targeting Mdm2, EMBO J. 26 (2007) 976–986.

[5] A.K. Hock, K.H. Vousden, The role of ubiquitin modification in the regulation of p53, Biochim. Biophys. Acta. 1843 (2014) 137–149.

[6] N. Allende-Vega, A. Sparks, D.P. Lane, M.K. Saville, MdmX is a substrate for the deubiquitinating enzyme USP2a, Oncogene. 29 (2010) 432–441

[7] E. Graner, D. Tang, S. Rossi, A. Baron, T. Migita, L.J. Weinstein, M. Lechpammer, D. Huesken, J. Zimmermann, S. Signoretti, M. Loda, The isopeptidase USP2a regulates the stability of fatty acid synthase in prostate cancer., Cancer Cell. 5 (2004) 253–261.

[8] X. Tong, K. Buelow, A. Guha, R. Rausch, L. Yin, USP2a Protein Deubiquitinates and Stabilizes the Circadian Protein CRY1 in Response to Inflammatory Signals, J. Biol. Chem. 287 (2012) 25280–25291.

[9] J. Shan, W. Zhao, W. Gu, Suppression of cancer cell growth by promoting cyclin D1 degradation., Mol. Cell. 36 (2009) 469–476.

[10] C. Priolo, D. Tang, M. Brahamandan, B. Benassi, E. Sicinska, S. Ogino, A. Farsetti, A. Porrello, S. Finn, J. Zimmermann, P. Febbo, M. Loda, The isopeptidase USP2a protects human prostate cancer from apoptosis., Cancer Res. 66 (2006) 8625–8632.

[11] T.S. Gansler, W. Hardman, D.A. Hunt, S. Schaffel, R.A. Hennigar, Increased expression of fatty acid synthase (OA-519) in ovarian neoplasms predicts shorter survival., Hum. Pathol. 28 (1997) 686–692.

[12] D.A. Hunt, H.M. Lane, M.E. Zygmont, P.A. Dervan, R.A. Hennigar, MRNA stability and overexpression of fatty acid synthase in human breast cancer cell lines., Anticancer Res. 27 (2007) 27–34.

[13] A. Baron, T. Migita, D. Tang, M. Loda, Fatty acid synthase: A metabolic oncogene in prostate

cancer?, J. Cell. Biochem. 91 (2004) 47–53.

[14] M. Renatus, S.G. Parrado, A. D'Arcy, U. Eidhoff, B. Gerhartz, U. Hassiepen, B. Pierrat, R. Riedl, D. Vinzenz, S. Worpenberg, M. Kroemer, Structural Basis of Ubiquitin Recognition by the Deubiquitinating Protease USP2, Structure. 14 (2006) 1293–1302.

[15] M.I. Davis, R. Pragani, J.T. Fox, M. Shen, K. Parmar, E.F. Gaudiano, L. Liu, C. Tanega, L. McGee, M.D. Hall, C. McKnight, P. Shinn, H. Nelson, D. Chattopadhyay, A.D. D'Andrea, D.S. Auld, L.J. DeLucas, Z. Li, M.B. Boxer, A. Simeonov, Small Molecule Inhibition of the Ubiquitin-specific Protease USP2 Accelerates cyclin D1 Degradation and Leads to Cell Cycle Arrest in Colorectal Cancer and Mantle Cell Lymphoma Models, J. Biol. Chem. 291 (2016) 24628–24640.

[16] K. Magiera, M. Tomala, K. Kubica, V. De Cesare, M. Trost, B.J. Zieba, N. Kachamakova-Trojanowska, M. Les, G. Dubin, T.A. Holak, L. Skalniak, Lithocholic Acid Hydroxyamide Destabilizes Cyclin D1 and Induces G 0 /G 1 Arrest by Inhibiting Deubiquitinase USP2a, Cell Chem. Biol. 24 (2017) 458–470.

[17] J. Angulo, P.M. Nieto, STD-NMR: application to transient interactions between biomolecules-a quantitative approach., Eur. Biophys. J. 40 (2011) 1357–69.

[18] B.-H. Lee, D. Finley, R.W. King, A High-Throughput Screening Method for Identification of Inhibitors of the Deubiquitinating Enzyme USP14., Curr. Protoc. Chem. Biol. 4 (2012) 311–330.

[19] R. Stoll, C. Renner, S. Hansen, S. Palme, C. Klein, A. Belling, W. Zeslawski, M. Kamionka, T. Rehm, P. Mühlhahn, R. Schumacher, F. Hesse, B. Kaluza, W. Voelter, R.A. Engh, T.A. Holak, Chalcone derivatives antagonize interactions between the human oncoprotein MDM2 and p53, 40 (2001) 336–344.

[20] L. D'Silva, P. Ozdowy, M. Krajewski, U. Rothweiler, M. Singh, T.A. Holak, Monitoring the effects of antagonists on protein-protein interactions with NMR spectroscopy, J. Am. Chem. Soc. 127 (2005) 13220–13226.

[21] D. Pal, P. Chakrabarti, Different Types of Interactions Involving Cysteine Sulfhydryl Group in Proteins, J Biomol Struct Dyn. 1102 (2017) 1059–1072.

[22] M. Mayer, B. Meyer, Characterization of Ligand Binding by Saturation Transfer Difference NMR Spectroscopy, Angew. Chemie Int. Ed. 38 (1999) 1784–1788.

[23] B. Meyer, T. Peters, NMR spectroscopy techniques for screening and identifying ligand binding to protein receptors., Angew. Chem. Int. Ed. Engl. 42 (2003) 864–890.

[24] P.J. Hajduk, J. Greer, A decade of fragment-based drug design: strategic advances and lessons learned., Nat. Rev. Drug Discov. 6 (2007) 211–219.

[25] C. Dalvit, NMR methods in fragment screening: theory and a comparison with other biophysical techniques., Drug Discov. Today. 14 (2009) 1051–1057.

[26] S.B. Shuker, P.J. Hajduk, R.P. Meadows, S.W. Fesik, Discovering high-affinity ligands for proteins: SAR by NMR., Science. 274 (1996) 1531–1534.

[27] C.W. Murray, M.L. Verdonk, D.C. Rees, Experiences in fragment-based drug discovery, Trends Pharmacol. Sci. 33 (2012) 224–232.

[28] E. Barile, M. Pellecchia, NMR-based approaches for the identification and optimization of inhibitors of protein-protein interactions., Chem. Rev. 114 (2014) 4749–4763.

[29] M.J. Harner, A.O. Frank, S.W. Fesik, Fragment-based drug discovery using NMR spectroscopy, J. Biomol. NMR. 56 (2013) 65–75.

[30] H. Chen, X. Zhou, A. Wang, Y. Zheng, Y. Gao, J. Zhou, Evolutions in fragment-based drug design: the deconstruction-reconstruction approach, Drug Discov. Today. 20 (2015) 105–113.

[31] M. Waki, J. Meienhofer, Efficient preparation of N.alpha.-formylamino acid tert-butyl esters, J. Org. Chem. 42 (1977) 2019–2020.

[32] D.E. Scott, M.T. Ehebauer, T. Pukala, M. Marsh, T.L. Blundell, A.R. Venkitaraman, C. Abell, M. Hyvönen, Using a fragment-based approach to target protein-protein interactions, Chembiochem. 14 (2013) 332–342.

[33] E. Beers, J. Callis, Utility of polyhistidine-tagged ubiquitin in the purification of ubiquitin-protein conjugates and as an affinity ligand for the purification of ubiquitin-specific hydrolases, J. Biol. Chem. 268 (1993) 21645–21649.

[34] D.A. Erlanson, Introduction to fragment-based drug discovery, Top. Curr. Chem. 317 (2012) 1–32.

[35] M. Piotto, V. Saudek, V. Sklenar, Gradient-tailored excitation for single-quantum NMR spectroscopy of aqueous solutions, J. Biomol. NMR. 2 (1992) 661–665.

[36] M.D. Hanwell, D.E. Curtis, D.C. Lonie, T. Vandermeersch, E. Zurek, G.R. Hutchison, Avogadro: an advanced semantic chemical editor, visualization, and analysis platform, J. Cheminform. 4 (2012) 1–17.

[37] O. Trott, A.J. Olson, AutoDock Vina: improving the speed and accuracy of docking with a new scoring function, efficient optimization, and multithreading., J. Comput. Chem. 31 (2010) 455–461.

Acknowledgements

This research has been supported by the (Grant Preludium UMO-2016/23/N/ST5/01588), from the National Science Centre, Poland (to MDT), (to TAH) by the UMO-2011/01/B/ST5/01744 and UMO-2014/12/W/NZ1/00457 grants from the National Science Centre, Poland, by the Project operated within the Foundation for Polish Science TEAM/2011-8/2 Program, co-financed by the EU European Regional Development Fund and the Marie Curie FP7-Reintegration-Grant within the 7th European Community Framework Programme and (to GD) UMO-2011/01/D/NZ1/01169 from the National Science Centre, Poland. The research was carried out with the equipment purchased thanks to the financial support of the European Regional Development Fund in the framework of the Polish Innovation Economy Operational Program (contract no. POIG.02.01.00-12-023/08). MS acknowledges support by the

Deutsche Forschungsgemeinschaft, SFB1035; MS and GP by the EU Horizon 2020 ITN network AEGIS.

Competing Financial Interests Statement

The authors declare no competing financial interests.

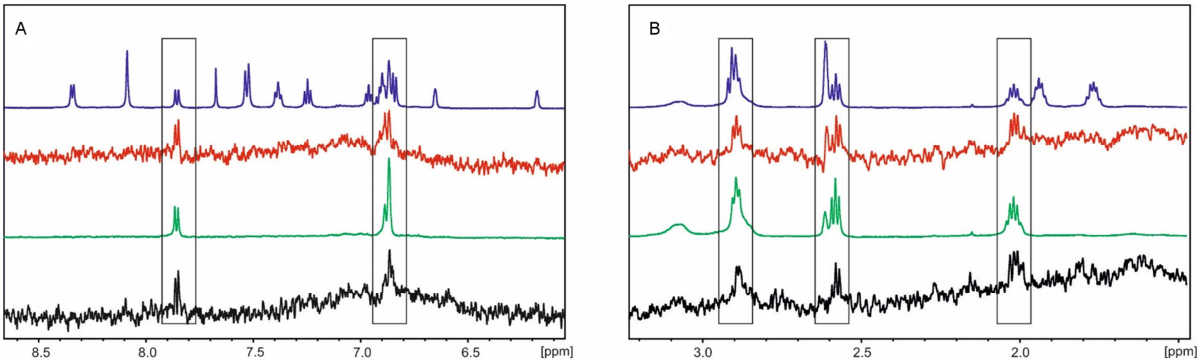

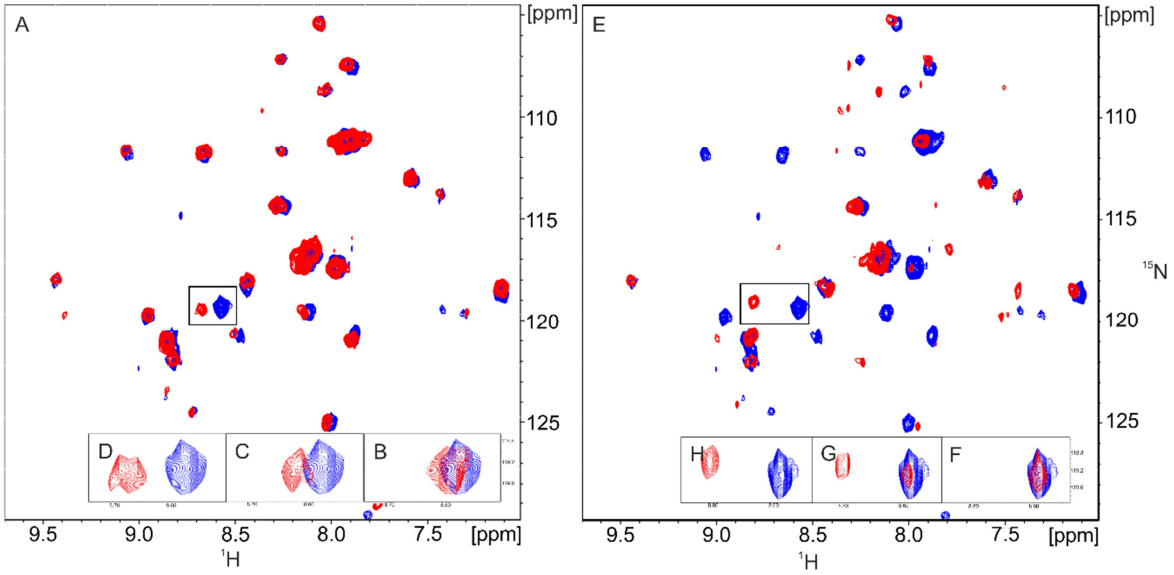

A

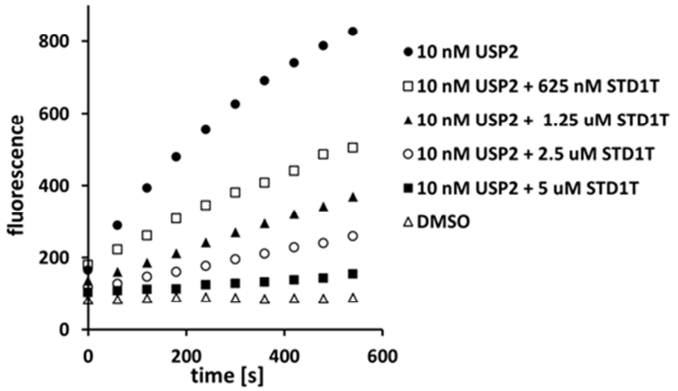

B

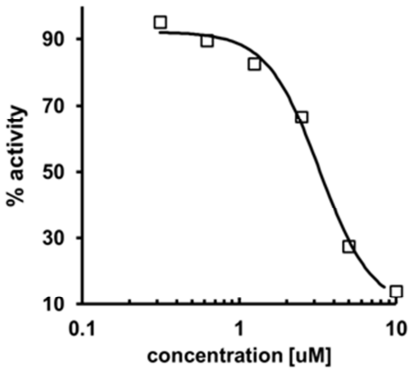

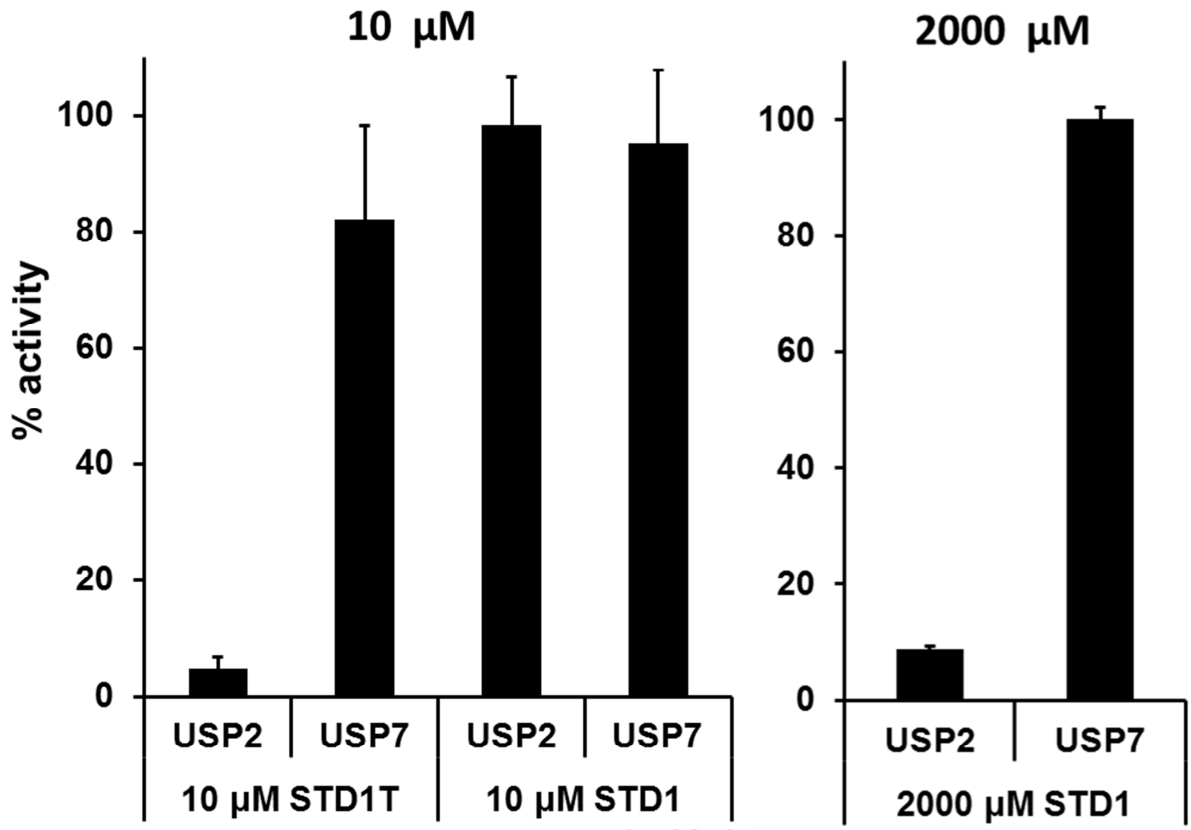

- Graphical Abstract has been corrected.
- The reference to the library used for STD screening assay was added to main text.
- The missing journal title in the literature position [21] was completed.
- The result of cell lines experiments has been included in the manuscript Supplementary Information.
- The figure Fig S4 that depicts the cell lines experiments was added to the manuscript Supplementary Information.
- The results of additional NMR measurements, required by the reviewers have now been included in a form of Fig S1 in Supplementary Information.
- The figure Fig 2 was corrected and added to manuscript Main Text according to the reviewer suggestions.
- The additional clarification of issues raised by the reviewers was added in the manuscript Main Text.
- The manuscript Main Text and Supplementary Information have been additionally checked in order to correct the language mistakes.